

Simple STM Tip Functionalization for Rapid DNA Sequencing: An Ab Initio Green's Function Study[†]

Ilya Yanov,[‡] J. J. Palacios,[‡] and Glake Hill^{*,‡}

Computational Center for Molecular Structure and Interactions (CCMSI), Department of Chemistry, Jackson State University, Jackson, Mississippi 39217, and Departamento de Física Aplicada, Universidad de Alicante, San Vicente del Raspeig, Alicante 03690, Spain.

Received: November 16, 2007; In Final Form: January 14, 2008

An ab initio nonequilibrium Green's function study of the electron-transport properties of the adenine, thymine, cytosine, and guanine DNA bases located between gold electrodes has been performed. One-electron transmission spectra were calculated for both gold and sulfur-modified gold electrodes, which are model conditions of scanning tunneling microscopy (STM) experiments with the different tips. It is shown that the nature of chemical bonding between molecules and metal electrodes plays the most significant role in the overall conductance of the systems. The distance between electrodes and the size of molecules are less important, at least when both sides of the molecule form chemical contact with the electrodes. On the basis of the obtained results, a simple two-pass DNA sequencing scheme is suggested.

Introduction

The possibility of utilization of DNA molecules as the building elements for molecular electronics has been largely discussed in the recent years due to the potential high density of its components, existing experimental techniques, and its double-strand recognition and self-assembly. Interestingly, one of the most important applications of molecular electronics is the sequencing of the DNA itself.

It has been believed that scanning tunneling microscopy (STM), break-junction, and nanopore techniques have a potential for rapid DNA sequencing by measuring the tunnel current between different DNA bases.^{1–4} However, experimental and theoretical results so far are controversial. Recent results show that tunnel current is mostly influenced by geometrical factors, such as the size of the DNA base and its orientation between electrodes, rather than by the nature of the base itself.⁴ To overcome those problems, it has been suggested to use STM tips modified by complementary DNA bases (Figure 1).⁵ It was found that the electron tunneling between a sample nucleobase and its complementary nucleobase molecular tip was much facilitated compared with its noncomplementary counterpart.⁵

Our early studies show that hydrogen bonds between complementary (A–T) base pairs indeed determine conductance at the Fermi level, but the absolute values of conductivity of such systems are very small.⁶ Besides, geometrical factors still will be very important. To use complementarity of the bases, it is necessarily to provide precise tip positioning and proper orientation of tip and substrate molecules.

In this paper, we show that simple functionalization of a gold STM tip by sulfur atoms can solve this problem. Moreover, only two STM tips (one gold tip and one gold–sulfur tip, Figure 2) will be necessary for sequencing the most common adenine (A), thymine (T), cytosine (C), and guanine (G) DNA base pairs.

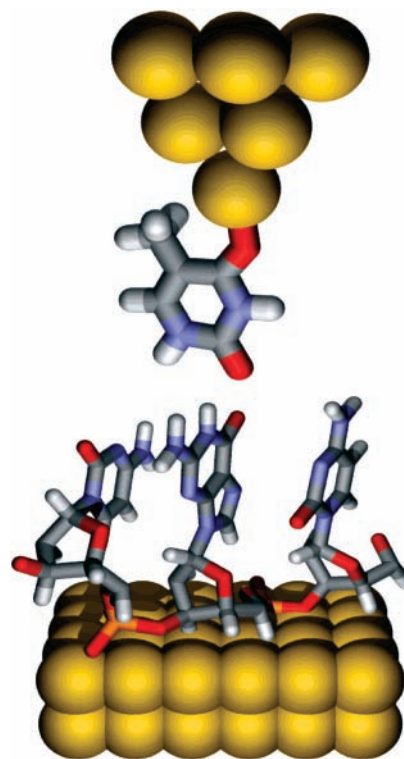


Figure 1. Scheme of the STM tip functionalization with the complementary DNA base.

Methods and Procedures

STM and break-junction experiments can be considered under the term molecular nanobridge, that is, a combination of a metallic electrode, a molecule, and a metallic electrode. The conductance G is essentially determined by the electronic structure of the isolated molecule (since the number of available transport channels for conduction deep in the electrodes is always much larger than those provided by the molecule) and

[†] Part of the "William A. Lester, Jr., Festschrift".

^{*} To whom correspondence should be addressed.

[‡] Jackson State University.

[‡] Universidad de Alicante.

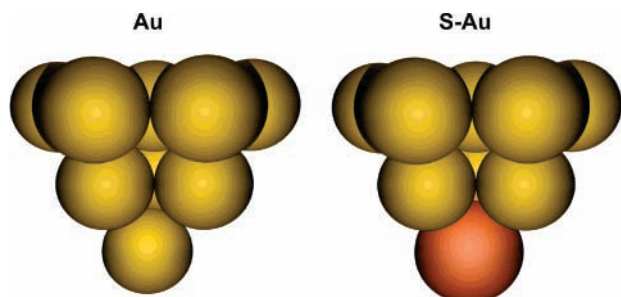


Figure 2. Gold and sulfur-gold tips.

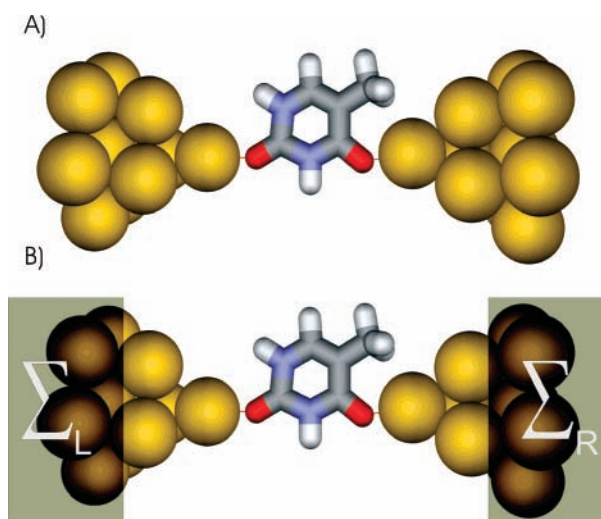


Figure 3. Schematic view of the two-step process for calculating the Green's function.⁷

by the chemistry of the electrode-molecule contacts.⁷ The necessity of aligning the Fermi level of the metallic electrodes with the “Fermi level” of the molecule forces a certain amount of charge to be transferred between an electrode and a molecule when they come in close proximity.⁸ Early work based on parametrized tight-binding or semiempirical models,⁹ where Fermi-level alignment has to be either entirely ignored or imposed with some additional criteria, has been superseded by *ab initio* Green's functions approaches in combination with Landauer formulation for the conductance.^{7,10–12} These approaches provide, in a natural manner, the correct alignment between the molecular levels and the density of states of the metallic electrodes.

One of the first theoretical models of STM imaging was proposed by Tersoff and Hamann.¹³ These authors consider the surface and tip as two separate systems and included tip-surface coupling by first-order perturbation theory using Bardeen's tunneling Hamiltonian and *s*-like wave functions for the tip.¹⁴ In this model, the STM tunnel current is proportional to the local density of states at the center of the tip, at the Fermi energy. The first nonperturbative treatment of STM imaging was reported by Lang¹⁵ in 1986. A Green's function formalism and jellium substrate model were employed. This simple substrate-tip model allowed significant insights into STM imaging and the near-point-contact regime, where perturbation theory is totally inadequate.¹⁰ In addition, the real atomic structure of the electrodes has been usually put aside. This is not satisfactory when one is trying to describe STM experiments, where the detailed atomic structure of the tip determines, to a large extent, whether or not the STM images can resolve the topography of

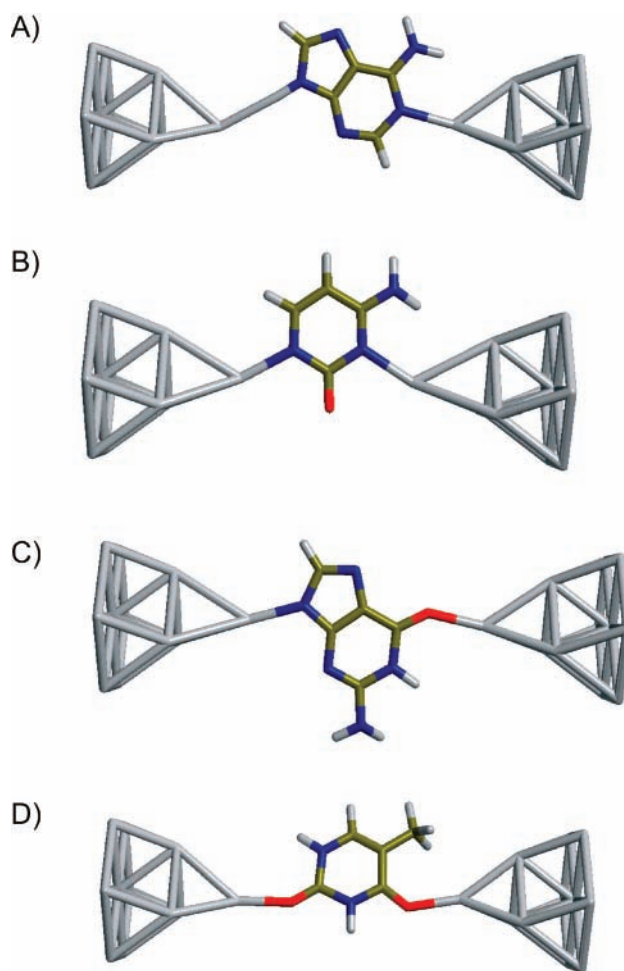


Figure 4. Scheme of DNA bases attached to the Au electrodes. (a) Adenine. (b) Cytosine. (c) Guanine. (d) Thymine.

the surface or the molecular structure of the adsorbate.⁷ Utilization of first-principles total-energy calculations as the part of the theoretical STM scheme allows also for automatic accounting of the surface-induced atomic relaxations on the tip as the latter is scanned.

In this project, we use the ALACANT code,⁷ which is based on the nonequilibrium Green's function formalism and works as an interface to GAUSSIAN program sets.¹⁶ Standard *ab initio* or quantum chemical calculations are only possible for finite or periodic systems, whereas the transport problem one typically wants to address requires infinitely large leads with no symmetry at all. The main idea here consists of performing a density functional (DF) calculation of the molecule including part of the leads with the desired geometry (see Figure 3a). This can be efficiently done using the GAUSSIAN03 code.¹⁶ For a sufficiently large number of atoms describing the metallic electrodes, the energy of the highest occupied molecular orbital of the whole structure sets the Fermi level. In addition, the correct charge transfer to or from the molecule is guaranteed. The Hamiltonian of the electrode-molecule-electrode system, \hat{H} as it stands, is finite, and according to the usual theoretical transport schemes,⁹ its Green's functions are unsuitable for any current determination since they have poles. In order to transform this finite system into an effectively infinite one, all but the N atoms forming the relevant atomic structure of each electrode close to the molecule were removed from the Hamiltonian (Figure 3b). The retarded Green's function associ-

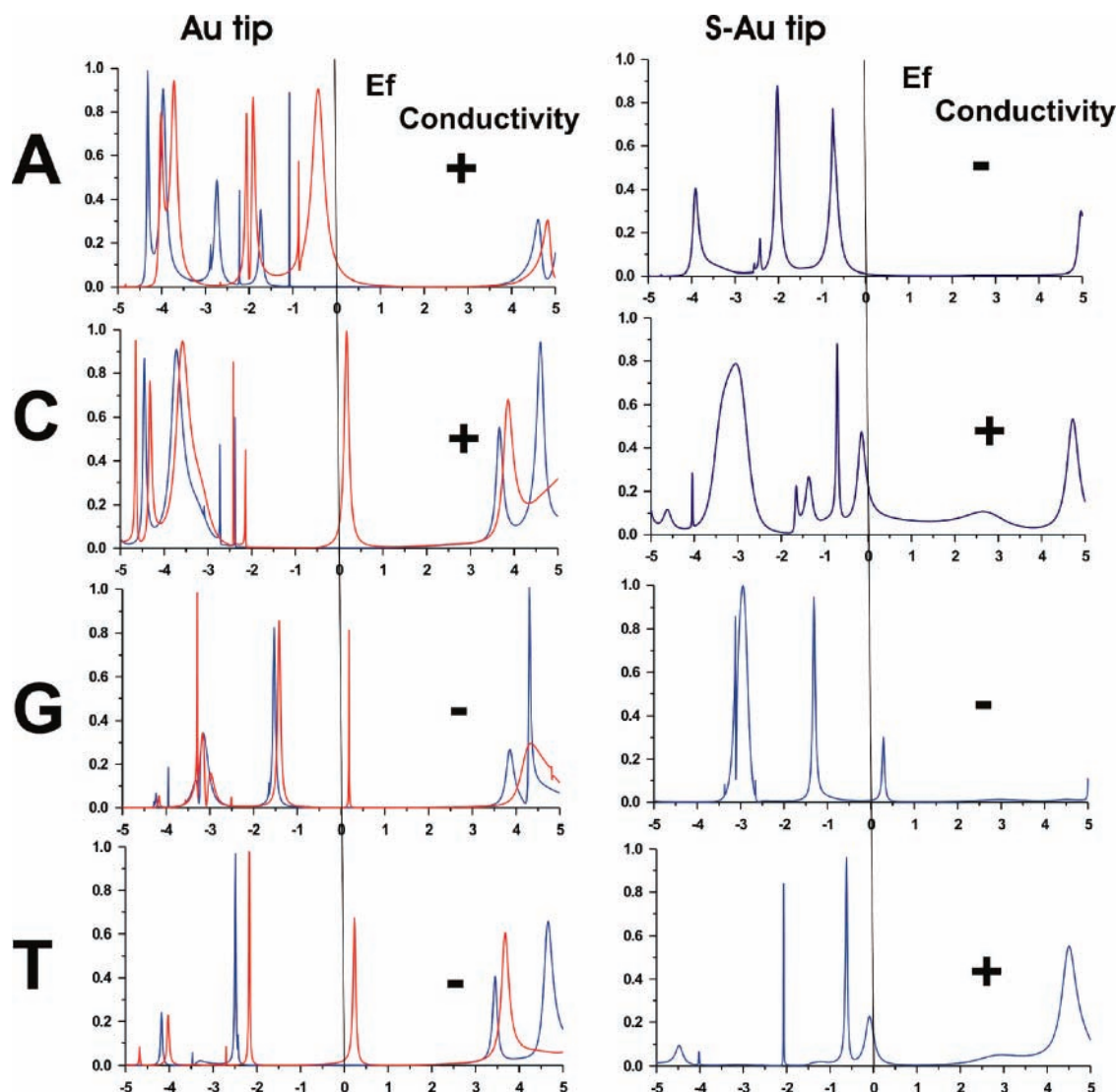


Figure 5. Transmission spectra of (A) adenine, (C) cytosine, (G) guanine, and (T) thymine molecules between gold electrodes. The blue color corresponds to alpha electrons; the red color indicates beta electrons. (Right side is for the gold–sulfur tip). Note: Alpha and beta transmissions degenerated for the gold–sulfur tip because of the closed shell of the system and the absence of a sizable charge transfer between the electrodes and molecule.

ated with this reduced Hamiltonian \hat{H}_r is now transformed into the retarded Green's function of an infinite system

$$G^r(\epsilon) = (\epsilon \hat{I} - \hat{H}_r + i\delta)^{-1} \rightarrow [\epsilon \hat{I} - \hat{H}_r - \hat{\Sigma}(\epsilon)]^{-1}$$

In this expression $\hat{\Sigma} = \hat{\Sigma}_R + \hat{\Sigma}_L$, where $\hat{\Sigma}_R(\hat{\Sigma}_L)$ denotes a self-energy matrix that accounts for the right (left) infinite electrode, part of which has been included in the DF calculation (Figure 3a).

When desired, the reduced Hamiltonian can be recalculated in a self-consistent manner. To this aim, the density matrix and the Fermi level can be obtained from the Green's function as usual⁷ and plugged back into GAUSSIAN to obtain the new reduced Hamiltonian.

The added self-energy can only be explicitly calculated in ideal situations. A number of groups in the field have chosen to model the bulk electrodes as perfect semi-infinite crystals.^{12,17,18} Since real electrodes are not monocrystals but polycrystalline structures with no expected long-range order beyond a few lattice constants, the atomic structure near the contact cannot possibly be perfect. In these models, the perfect

crystal band structure necessarily reflects in the final conductance of a molecule. Alternatively, jellium models are used in methods based on a description in terms of scattering states.^{19,20} This is also a choice of convenience not free from controversy.²¹ ALACANT describes the bulk electrode with a Bethe lattice-parametrized tight-binding model with the coordination and parameters appropriate for the chosen electrode (part of which has already been included in the cluster). The advantage of choosing a Bethe lattice resides in that, although it does not have long-range order, the short-range order is captured, and it reproduces fairly well the bulk density of states of most commonly used metallic electrodes. Assuming that the most important structural details of the electrode are included in the central cluster, the Bethe lattices should have no other relevance than that of introducing the most generic bulk electrode for a given metal. Bethe lattice can be easily calculated through a computationally efficient iteration procedure.^{22,23}

Assuming that the initial system is large enough and that the reduced system still contains the relevant atomic details of the electrode close to the contact with the molecule, effective self-energy should introduce no spurious effects, and it makes the

system effectively infinite. The conductance can be calculated through the expression⁹

$$G = \frac{2e^2}{h} \text{Tr}[\Gamma_L G^r \Gamma_R G^a]$$

where Tr denotes the trace over all of the orbitals of the reduced Hamiltonian and the matrices Γ_R and Γ_L are given by $i(\Sigma_R^r - \Sigma_R^a)$ and $i(\Sigma_L^r - \Sigma_L^a)$, respectively. In summary, this approach allows for (1) an ab initio quantum chemical description of the systems consisting of part of the tip–molecule part of the substrate, including study of atomic rearrangement on the surface in the presence of tip, (2) current–voltage spectroscopy for a finite bias voltage based on the nonequilibrium Green’s function formalism,²⁴ and (3) both spin-restricted and spin-unrestricted calculations.⁸

The combination of the ab initio nonequilibrium Green’s function formalism, the ability for spin-polarized calculations, and the computational effectiveness makes the ALACANT implementation unique among available methods.

Results and Discussion

The scheme of the electric circuit where adenine (A), thymine (T), cytosine (C), and guanine (G) DNA bases are chemically bound to the Au model contacts is shown in Figure 4a–d. We start by optimizing gold electrode–DNA base systems at the B3LYP/STO-3G level of theory using the GAUSSIAN03¹⁷ program set. Unlike break-junction experiments, where the distance between electrodes is fixed, we would like to compare the conductivity of DNA bases in the presence of similar chemical contacts with the electrodes. Therefore, the second electrode is placed on the other side of the system at the optimal distances (2.16–2.17 Å) from the terminal N and O atoms. No further optimization is performed. Christiansen core pseudopotentials described in refs 25–27 are used for Au atoms.

The results of the calculations of transmission spectra for the considered systems are presented in Figure 5. It is shown (Figure 5A,C, left side) that adenine and cytosine molecules exhibit significant conductance at small voltage biases. (According to Landauer’s formalism, $G(E_f) = (2e^2/h)T(E_f)$, where $T(E_f)$ denotes the total transmission of all of the conductance channels at the Fermi energy.) The conductance of both molecules is very similar at the Fermi level but exhibits asymmetry when a bias voltage is applied. For positive values of the bias, the conductance of adenine decreases, as well as the conductance of cytosine for a negative bias voltage. The conductance of thymine is much lower and almost vanishes for guanine (Figure 5G,T). Taking into account similar delocalization of the HOMO and LUMO orbitals and the similar size of adenine and guanine molecules, we can assume that the changes of conductance are due to the influence of the oxygen atoms on the molecule–electrode interface. The same conclusion can be obtained for cytosine and thymine. It is of interest that in both A–T and G–C base pairs, one part of the pair (A or C) has significantly better conductivity near the Fermi level.

Transmission spectra of the systems, where the top gold atom of the STM tip is replaced by a sulfur atom, are presented in Figure 5 (right side). It is shown that the conductivity of the bases changes significantly. The conductivity of adenine vanishes, while the conductivity of thymine rises. Therefore, if we consequently scan the same single-stranded oligonucleotide using both (gold and gold–sulfur) tips, it is possible to create

simple rules for sequencing DNA bases:

STM tip	adenine	cytosine	guanine	thymine
gold	+ ^a	+ ^a	–	–
gold–sulfur	–	+ ^a	–	+ ^a

^a The “+” signs here indicates that the “tip–DNA base–gold substrate” system exhibits conductance at the Fermi level.

It should also be noted that performing spin-unrestricted calculations is essential to obtain the correct splitting of the original molecular levels as the orbitals get filled or emptied by the electrodes in the self-consistent alignment of the molecular levels and the Fermi energy of the metal.⁸ This is of particular relevance when the molecular orbitals are weakly coupled to the electrodes, as is the case here, and charge localization is strong (note that the use of hybrid functionals here like B3LYP is crucial to partially avoid self-interaction effects⁸). It is not uncommon that spin-restricted calculations result in a transmission peak near the Fermi level. In such a case, failure in considering spin-unrestricted calculations can lead to a highly overestimated conductance, as we recently showed for the case of the gold–porphyrin–gold system.²⁸

Summary

In this paper, we have discussed the electron-transport properties of the adenine (A), thymine (T), cytosine (C), and guanine (G) DNA bases between gold contacts. Calculations were performed using DFT theory and the nonequilibrium Green’s function formalism with the help of the ALACANT code.

It was revealed that one of the most important factors which influence the overall conductance of the DNA bases is the specific characteristics of chemical bonding between molecules and metal electrodes. The distance between electrodes is less important, at least when both sides of the molecule form a chemical contact with the electrodes. Systems where the gold electrode–molecule interface involves one or two oxygen molecules exhibit the lowest conductance.

The scheme of rapid DNA sequencing based on gold and gold–sulfur tips is provided. The importance of spin-unrestricted calculations has been shown. Spin-restricted models significantly overestimate conductance.

Acknowledgment. This work was supported by the Department of Defense through the U.S. Army Engineer Research and Development Center (Vicksburg, MS), Contracts #W912HZ-04-2-0002 and #W912HZ-05-C-0051, and NSF-PREM Grant # DMR-0611539. J.J.P. acknowledges financial support from MEC of Spain under Grants Nos. MAT2007-65487 and CSD2007-0010.

References and Notes

- (1) Kanno, T.; Tanaka, H.; Miyoshi, N.; Fukuda, M.; Kawai, T. *Jpn. J. Appl. Phys.* **2000**, *39*, 1892.
- (2) Zwolak, M.; Di Ventra, M. *Nano Lett.* **2005**, *5*, 421.
- (3) Lagerqvist, J.; Zwolak, M.; Di Ventra, M. *Nano Lett.* **2006**, *6*, 779.
- (4) Zhang, X.-G.; Krstic, P. S.; Zikic, R.; Wells, J. C.; Fuentes-Cabrera, M. *Biophys. J.* **2006**, *91*, L04.
- (5) Ohshiro, T.; Umezawa, Y. *Proc. Natl. Acad. Sci.* **2006**, *103*, 10.
- (6) Yanov, I.; Leszczynski, J. *Int. J. Quantum Chemistry* **2004**, *96*, 436.
- (7) (a) Palacios, J. J.; Pérez-Jiménez, A. J.; Louis, E.; Vergés, J. A. *Phys. Rev. B* **2001**, *64*, 115411. (b) Palacios, J. J.; Pérez-Jiménez, A. J.; Louis, E.; SanFabián; Vergés, J. A. *Phys. Rev. B* **2002**, *66*, 035322. (c) For more information on the code, visit the webpage: ALACANT. www.dfa.ua.es/en/invest/condens/Alacant/.
- (8) Palacios, J. J. *Phys. Rev. B* **2005**, *72*, 125424.

- (9) For references, see: Datta, S. In *Electronic Transport in Mesoscopic Systems*, Ahmed, H., Pepper, M., Broers, A., Eds.; Cambridge University Press: Cambridge, England, 1995.
- (10) Di Ventra, M.; Pantelides, S. T. *Phys. Rev. B* **1999**, *59*, 5320.
- (11) Lang, N. D.; Avouris, Ph. *Phys. Rev. Lett.* **1998**, *81*, 3515.
- (12) Taylor, J.; Guo, H.; Wang, J. *Phys. Rev. B* **2001**, *63*, 121104.
- (13) Tersoff, J.; Hamann, D. R. *Phys. Rev. Lett.* **1983**, *50*, 1998.
- (14) Bardeen, J. *Phys. Rev. Lett.* **1961**, *6*, 57.
- (15) Lang, N. D. *Phys. Rev. Lett.* **1986**, *56*, 1164.
- (16) Frisch, M. J.; Trucks, G. W.; Schlegel, H. B.; Scuseria, G. E.; Robb, M. A.; Cheeseman, J. R.; Montgomery, J. A., Jr.; Vreven, T.; Kudin, K. N.; Burant, J. C.; Millam, J. M.; Iyengar, S. S.; Tomasi, J.; Barone, V.; Mennucci, B.; Cossi, M.; Scalmani, G.; Rega, N.; Petersson, G. A.; Nakatsuji, H.; Hada, M.; Ehara, M.; Toyota, K.; Fukuda, R.; Hasegawa, J.; Ishida, M.; Nakajima, T.; Honda, Y.; Kitao, O.; Nakai, H.; Klene, M.; Li, X.; Knox, J. E.; Hratchian, H. P.; Cross, J. B.; Bakken, V.; Adamo, C.; Jaramillo, J.; Gomperts, R.; Stratmann, R. E.; Yazyev, O.; Austin, A. J.; Cammi, R.; Pomelli, C.; Ochterski, J. W.; Ayala, P. Y.; Morokuma, K.; Voth, G. A.; Salvador, P.; Dannenberg, J. J.; Zakrzewski, V. G.; Dapprich, S.; Daniels, A. D.; Strain, M. C.; Farkas, O.; Malick, D. K.; Rabuck, A. D.; Raghavachari, K.; Foresman, J. B.; Ortiz, J. V.; Cui, Q.; Baboul, A. G.; Clifford, S.; Cioslowski, J.; Stefanov, B. B.; Liu, G.; Liashenko, A.; Piskorz, P.; Komaromi, I.; Martin, R. L.; Fox, D. J.; Keith, T.; Al-Laham, M. A.; Peng, C. Y.; Nanayakkara, A.; Challacombe, M.; Gill, P. M. W.; Johnson, B.; Chen, W.; Wong, M. W.; Gonzalez, C.; Pople, J. A. *Gaussian 03*; Gaussian, Inc.: Pittsburgh, PA, 2003.
- (17) Brandbyge, M.; Mozos, J. L.; Ordejon, P.; Taylor, J.; Stokbro, K. *Phys. Rev. B* **2002**, *65*, 165401.
- (18) Damle, P. S.; Ghosh, A. W.; Datta, S. *Phys. Rev. B* **2001**, *64*, 201403.
- (19) Lang, N. D. *Phys. Rev. B* **1995**, *52*, 5335.
- (20) Hirose, K.; Tsukada, M. *Phys. Rev. B* **1995**, *51*, 5278.
- (21) Fujimoto, Y.; Hirose, K. *Phys. Rev. B* **2003**, *67*, 195315.
- (22) Martín-Moreno, L.; Vergés, J. A. *Phys. Rev. B* **1990**, *42*, 7193.
- (23) Joannopoulos, J. D.; Yindurain, F. *Phys. Rev. B* **1974**, *10*, 5164.
- (24) Louis, E.; Vergés, J. A.; Palacios, J. J.; Pérez-Jiménez, A. J.; SanFabián, E. *Phys. Rev. B* **2003**, *67*, 155321.
- (25) Pacios, L. F.; Christiansen, P. A. *J. Chem. Phys.* **1985**, *82*, 2664.
- (26) Hurley, M. M.; Pacios, L. F.; Christiansen, P. A.; Ross, R. B.; Emler, W. C. *J. Chem. Phys.* **1986**, *84*, 6840.
- (27) Ross, R. B.; Powers, J. M.; Atashroo, T.; Emler, W. C.; LaJohn, L. A.; Christiansen, P. A. *J. Chem. Phys.* **1990**, *93*, 6654.
- (28) Yanov, I.; Kholod, Y.; Leszczynski, J.; Palacios, J. J. *Chem. Phys. Lett.* **2007**, *445*, 238.